

# 14<sup>th</sup> International Conference on Jetting Technology Brugge, Belgium: September 21-23 1998

## NUMERICAL ANALYSIS OF PULSED JET FORMATION BY ELECTRIC DISCHARGES IN A NOZZLE

M.M. Vijay and A.H. Makomaski\*\*

<sup>v</sup>L<sub>N</sub> Advanced Technologies, Inc.

(Formerly Centre for Fluid Power Technology, National Research Council)

P.O. Box 27076, Gloucester Centre Postal Outlet

Gloucester, ON., Canada, K1J 9L9

Fax: (613) 952-1395

E-Mail: mohan.vijay@nrc.ca

\*\* Consultant

2257 Prospect Avenue, Ottawa, ON., Canada

### SYNOPSIS

In order to complement experiments and improve understanding of the phenomena accompanying electrical discharges in a nozzle, a numerical approach was applied. Major attention was focused on the creation of single-pulse water jets, although some preliminary study was conducted on the transient acceleration of a continuous water jet. The numerical method involved a two-dimensional Lagrangian formulation in cylindrical coordinates. Effect of variables, such as electrode location in the nozzle, was examined. It is shown that the numerical code does confirm the formation of a pulse of water following the electrical discharge. Based on this work, suggestions for further study are put forward.

### 1.0 INTRODUCTION

Figures 1 and 2 show the two high-voltage electro-discharge experimental systems under investigation for producing powerful pulsed water jets. Figure 1 consists of modulating a stream of water with high-voltage discharges. No details on this configuration will be given here as Vijay, et. al (Ref. 1) have given ample description, including all the problems (and solutions) that accompany high-voltage discharge in a nozzle. Likewise the system shown in Fig. 2 (this is similar to a water cannon) will not be described here as the details have been reported by Vijay, et.al (Ref. 2). Although the electro-discharge (or, electro-hydraulic) technique is known for a number of years (Refs. 3 & 4; these references also contain an extensive bibliography on the topic), it is only recently that systematic approach for producing pulsed jets has been reported (Refs. 1, 2, 5, 6 & 7). A variation of the technique, generally known as "plasma blasting", has also been investigated for mining (Refs. 8 & 9) and safe blasting of rock formations (Ref. 10).

Briefly, when a high voltage is discharged between the electrodes in a nozzle (see Fig. 1), an electric arc is formed. As described in Ref. 1, the voltage required to induce the arc depends,

among other factors, on the quality of water and the distance between the electrodes (usually 3.6 kV/mm of gap width in tap water). The duration of the electrical discharge is a function of the electrical circuit parameters (capacitance, inductance and resistance) and could last from 5 to 400  $\mu$ s. The discharge generates a shock wave and a plasma bubble that could attain a maximum diameter of 10 mm in about 1  $\mu$ s. According to Huff & McFall (Ref. 11), the cutting ability of the jet is augmented by three mechanisms: (1) the initial shock wave, (2) pulsed jet produced by the shock wave or, rapidly expanding plasma bubble and (3) the plasma bubble itself which eventually reverts into a cavitation bubble. In practice, however, it is not possible to achieve all three effects in a single nozzle. It is much easier to design a nozzle for achieving a single effect, for example, shock wave induced pulsed jet. As the time required to charge the capacitors is usually quite long compared to the discharge time, the frequency of operation is usually quite low ( $\approx$  0.5 Hz).

It is clear from the description given above that the electro-discharge technique is a multi-disciplinary subject, spanning from pulsed electrical discharges, plasma (bubble) physics to highly complex shock wave propagation. Due to this complexity, it is not possible to derive theoretical solutions to account for all the phenomena accompanying the discharge. No numerical code (computational fluid dynamics analysis code) exists to solve the problem in its entirety, although Atanov and his colleagues (Refs. 6 & 7) have made some efforts to track the problem. In their first study (Ref. 6), the authors solved numerically a set of differential equations (continuity, etc.) to predict the speeds of water jet and the contact surface (plasma bubble - water interface). As shown in Fig. 3, both speeds have two maxima. The explanation for this occurrence is as follows: Immediately after the discharge, a shock wave detaches from the cavity (plasma bubble) surface. While moving along the converging section, its strength is augmented with the consequent rise in pressure and speed of water behind it. However, the pressure in the cavity and the speed of its surface decrease. When the shock wave arrives at the nozzle exit, the water is ejected and the rarefaction wave travels upstream towards the cavity. The subsequent interaction between the cavity surface and the rarefaction wave leads to the acceleration of the former leading to the generation of a new compression wave in the water. Arriving at the nozzle exit, this wave contributes to the increase of water jet speed. The first maximum in the cavity surface speed is due to the deposition of electrical energy.

It appears that in the study described above, the authors considered interruption of quiescent water in a nozzle, similar to the configuration shown in Fig. 2. In the more recent study (Ref. 7), they analyzed the interruption of a steady flow with electric discharges (Fig. 4a; similar to Fig. 1). To obtain the water jet velocity, the authors used a set of differential equations in which sonic speed of water (instead of density) and the water velocity appeared as dependent variables. They solved the equations numerically and plotted the speed of water at the outlet of the nozzle as a function of time (Fig. 4b). The reasons for the fluctuating character of the outlet speed were attributed, as shown in Fig. 4a, to the propagation of shock waves from the point of discharge to the nozzle exit, their reflection and interaction with the cavity surface, etc. The authors did not support their theoretical predictions with experimental results.

Although the work of Atanov, et. al (Refs. 6 & 7) generally support the experimental results reported by Vijay, et. al (Refs. 1 & 2), it is not enough to fully understand the physics of the electro-discharge process and the mechanism of pulsed jet formation. As explained earlier, the process is quite complex and is influenced by many configurational (nozzle geometry, electrode geometry, gap and location with respect to nozzle exit, etc), electrical parameters (energy, duration of discharge, etc) and operating variables (static pressure and flow). The purpose of the preliminary numerical analysis presented in this paper is to complement the experimental work

which is in progress (Refs. 1 & 2) and to improve the understanding of phenomena accompanying creation of single-pulse jets and transient acceleration of continuous jet by electrical discharges.

## 2.0 THEORY

In experiments, as shown in Fig. 5, ABCD represents an axisymmetric nozzle with the exit plane at DC. AB can be either an inflow plane (for continuous jets; see Fig. 1) or, the solid wall (for single-pulse jets; see Fig. 2). Electrical discharge taking place between two electrodes creates a high-pressure, high-density plasma which generates a strong spherical shock wave into the water contained by ABCD. The part of the shock wave directed towards DC accelerates water to create a transient high speed jet through the exit plane DC.

The numerical method involves a two-dimensional Lagrangian formulation in cylindrical coordinates. Water is assumed to be a slightly compressible medium and the plasma resulting from the electrical discharge into water is approximated by water vapour, which is assumed to behave as an ideal gas. The assumption of two-dimensionality requires the numerical "plasma" to be in the shape of a disc. The relevant equations relating to water and water vapour are as follows:

Conservation of mass:

$$\rho J = \rho_0 J_0 \quad (1)$$

Equation of motion:

$$\rho \frac{\partial V}{\partial t} = -\nabla p + Q_1 \quad (2)$$

Conservation of energy:

$$\frac{\partial e}{\partial t} = -p \frac{\partial \tau}{\partial t} + \frac{\partial E}{\partial t} + Q_2 \quad (3)$$

Equation of state for water:

$$p = (p_0 + B) \left\{ \frac{\rho}{\rho_0} \right\}^{7.15} - B \quad (4)$$

where:  $B = 3010$  atm.

Equation of state of water vapour - assumed as an ideal gas:

$$p = \rho e (\gamma - 1) \quad (5)$$

where  $\gamma = 1.33$

In the above equations  $J$  is a volume Jacobian of transformation,  $\rho$  is density,  $p$  is pressure,  $\underline{V}$  is velocity,  $\tau$  is specific volume,  $e$  is internal energy,  $E$  is energy deposited in plasma by electrical discharge and  $Q_1$  and  $Q_2$  are terms connected with an artificial viscosity with directional properties (Ref. 12). The subscript 0 indicates initial conditions (here at atmospheric pressure).

Although knowledge of internal energy of water is not required in the computations, it is nonetheless calculated to keep track of energy balance (sum of kinetic energy and internal energy for both water and plasma versus energy added by the electrical discharge).

### 3.0 DEVELOPMENT OF THE CODES

Two codes were developed whose functions were:

- a. To compute single-pulse jets (**CODE WATER4.F**);
- b. To study electrical discharges into a steady flow (**CODE WATER5.F**).

In both cases the geometry, shown in Fig. 6, was set up by specifying radii R1, R2 and R3 and distances ZSTR, ZPASS and ZOUT along the axis (R and Z are cylindrical coordinates). All these dimensions are in cm. The shape of the converging section was calculated automatically from the above dimensions. The outline of the converging section was designed to be tangential at B and C to the straight parts of the chamber and the nozzle.

The numerical grid was set up in dimensionless Lagrangian coordinates K and L running respectively in the radial and axial directions. The discharge volume was set up by specifying KFEED, LFEED and LFEEDL on the assumption that the discharge volume 'A' had the shape of a disc. Its volume was adjusted to be approximately the same as the estimated volume of the discharge column between the two electrodes.

The numerical time increments  $\Delta T$  could be calculated as computations proceed, but the practice was to estimate  $\Delta T$  for the smallest numerical zones and then to use this constant value throughout the calculation.

In the present investigation the following phenomena were studied:

- a. Effect of location of discharge plasma (single-pulse jets);
- b. Local high velocities in the jet (single-pulse jets);
- c. Mechanism of water break-up and formation of the water "bullet" leaving the nozzle (single-pulse jets);
- d. Acceleration of issuing jet due to electrical discharge in a steady flow (very limited results are presented here).

### 4.0 COMPUTATION OF SINGLE-PULSE JETS (CODE WATER4.F)

To set up the problem the chamber and the nozzle were filled with water at atmospheric pressure. Before energy was added to volume A, water in that volume was assumed to change to water vapour having the same mass as the mass of the water occupying volume A.

It is assumed that electrical energy ( $E_{el}$  in kJ) is added to A in time  $T_D$  ( $\mu s$ ) at a constant rate with efficiency  $E_{eff}$  giving the rate of energy addition of  $E_t = E_{eff} \times E_{el} / T_D$  for the time period  $T_D$ . This energy is added incrementally to the internal energy of water vapour in A, needed for the calculation of pressure.

#### 4.1 Effect of Location of the Discharge Plasma

Figure 7 shows the distribution of densities (density gradient) after discharge in the nozzle configuration of Fig. 2. In Fig. 7(A) the electrodes are located away from the back wall (experimental set-up investigated in Ref. 2) and in Fig. 7(B), they are very close to the back wall. The results clearly indicate that the discharge volume (electrodes) should be located as close to the back wall of the chamber as possible. The energy in the shock propagating upstream of the electrodes in (A) does not contribute to the acceleration of water. Disposition of the electrodes close to the back wall allows the electrical energy to be used to accelerate the water towards the nozzle exit, resulting in a significant increase in jet velocity. The magnitudes of the speed estimated by the code at 135  $\mu\text{s}$  after discharge ( $E_{el} = 3.5 \text{ kJ}$ ) were 424 m/s and 574 m/s respectively for (A) and (B). Although most single-pulse calculations were carried out with plasma at the back wall of the chamber, it should be noted that in practice it is not possible to locate the electrodes very close to the back wall due to tracking and other problems (Ref. 1).

#### 4.2 Local High Velocities

The analysis showed that high local jet velocities (origins of precursors?) exist at jet tips. The magnitude of these was observed to depend on:

- a. Efficiency of the electrical system;
- b. Length of constant-diameter part of the exit nozzle (ZOUT in Fig. 6);
- c. Length of the chamber ( $Z_{LONG} = Z_{STR} + Z_{PASS}$  in Fig. 6).

A summary of results is given in Fig. 8. It is seen that for small ZOUT ( $0.224 \leq Z_{OUT} \leq 0.895$ ) there is a large jump in the magnitude of the precursor. This jump is not reflected in average velocities through the nozzle. Although it is difficult to explain the mechanism of formation of precursors, Rochester & Brunton (Ref. 13), using high speed photography, have shown that they exist. The high values, of the order of 1000 m/s, measured by Vijay, et. al (Ref. 2) are probably due to the precursors.

#### 4.3 Formation of the Water “Bullet”

The electro-discharge nozzle, in many ways, is similar to the shock tube except for the varying geometry and, much can be learned from the extensive work that has been done on shock tubes (Ref. 14). Immediately after the deposition of energy between the electrodes, a series of compression waves coalesce to form a hemispherical shock wave. This can be clearly seen in Fig. 9(A) where contours of constant density are depicted 10  $\mu\text{s}$  after the discharge ( $E_{el} = 3.5 \text{ kJ}$ ). As expected density increases gradually behind the shock front from a value of about 1.02 to about 1.07  $\text{kg/m}^3$  at the bubble-water interface, particularly close to the axis. Subsequently, as the shock wave propagates at high speed, the transient wave phenomena, wave structure and wave interactions become quite complex as shown in Figs. 9(B) to 9(F). For instance, Fig. 9(B) shows the reflection of the incident wave from the nozzle wall (indicated by “c”). This reflected wave trails behind the incident wave (indicated by “b”) and upon reaching the axis is reflected back towards the wall [indicated by “c” near the bubble in Fig. 9(C)]. The net result of these multiple interactions is that the shock wave becomes planar as it progresses downstream. On reaching the convergent part, the incident shock again reflects, at first as a Mach reflection and later as regular

reflection. Finally, it becomes gradually stronger as it moves through the converging part to the nozzle exit.

When the shock arrives at the nozzle exit, it is reflected as an expansion wave which, traveling upstream, will begin to reduce the pressure (diffraction and refraction also occur which are not considered here). A search method was introduced to detect the low pressure region in the chamber where separation of the high speed jet “bullet” leaving the nozzle, from the water remaining in the chamber, is expected to occur. In this region water is under tension as defined by a reversal of direction of local axial velocity, i.e., axial velocity points outwards on opposite sides of an element of water. The method was mostly applied to the case of the experimental energy release and discharge efficiency (3.5 kJ and 20%; Ref. 2). It was concluded that the kinetic energy of the “bullet” is about 20% of the energy fed into the fluid and this is independent of the total length of the nozzle (ZSTR + ZPASS + ZOUT in Fig. 6; 8.95 cm and 18.1 cm lengths tested). For comparative purposes only a coarse grid was employed. The results were:

- a. Short nozzle (8.95 cm): bullet mass = 3.2 gm, mean velocity = 302 m/s;
- b. Long nozzle (18.1 cm): bullet mass = 4.3 gm, mean velocity = 261 m/s.

The expected region of separation occurred at about 90  $\mu\text{s}$  as indicated by the zigzag line in Fig. 9(F). The streaks in the jet are probably due to numerical difficulties arising from the lack of a suitable  $p/\rho$  relationship at atmospheric conditions. The method was also applied to much higher energies. It was found, however, that much greater care had to be taken of the region of the contact surface between the driving plasma and the driven water.

The code also included steps to verify how well energy was conserved in the flow system at various times (T) after the discharge. The results, summarized below, show that the energy was conserved quite well up to 70  $\mu\text{s}$  (that is, prior to the moment of water break-up). This observation suggests that refinements in the numerical code are required to accurately predict the break-up mechanism.

T ( $\mu\text{s}$ )	0.00	10.0	20.0	30.0	40.0	50.0	60.0	70.0	80.0	90.0
$\epsilon$ (%)	---	2.44	1.43	0.43	0.28	0.37	-0.17	-0.85	35.6	36.0

[ $\epsilon = (E_{\text{dis}} - \Sigma E)/E_{\text{dis}}$ ;  $E_{\text{dis}}$  = electrical energy deposited into the fluid,  $\Sigma E$  = total internal energy (IE) of the system (plasma as well as the water) + total kinetic energy KE]

## 5.0 STEADY FLOW WITH ELECTRIC DISCHARGE (CODE WATER5.F)

This version of the code was based on water4.f with the addition of a method of setting up steady flow through the chamber (left-end open; in practice, a check valve is located at the left-end) and the nozzle prior to the commencement of electrical discharge.

The first step was to assume an outlet velocity through the nozzle. Then, an approximate distribution of velocity, pressure and density was calculated in the chamber and the nozzle using 1-D assumptions. If  $V_{\text{IN}}$  is the resulting axial velocity at the left end, then this inlet velocity was assumed to be constant with radius (at inlet) and with time. This constant inlet velocity acts as a “piston” driving the flow in the chamber. Calculation was carried out in time until satisfactory distribution of flow parameters was obtained throughout the chamber and nozzle. At this moment energy can be deposited at any arbitrary place in the chamber.

Typical results (only preliminary at this point) for larger powers (14 kJ and 50 % efficiency; the experimental system is rated for 20 kJ) are given in Fig. 10 as density distributions for times

10, 20, 30, 40 and 60  $\mu\text{s}$  after commencement of discharge. For the sake of illustration, large energy deposition has been used because density variations were quite small at 3.5 kJ (static pressure in the nozzle was well above the atmospheric pressure). Based on the observations made in the case of single-pulse jet, it can be concluded that the shock induced by the discharge augments the acceleration of water contributing to higher jet velocities.

## 6.0 CONCLUSIONS

In the present study emphasis was placed on those aspects of numerical work which would assist in understanding experimental results. Thus, two aspects were covered: (a) the mechanism of creation of water “bullet” by break-up of flow in the chamber, and (b) discharge into a continuous flow. For example, the analysis has clearly shown the importance of the location of the electrodes in the nozzle chamber and the occurrence of high-speed precursors, qualitatively supporting the experimental results reported by Vijay, et.al (Ref. 2). The two versions of the code form a good basis for further study and optimization of single-pulse and continuous jets with electrical discharge. The implementation of the code will accelerate the development of the electro-discharge nozzle by minimizing the experimental work.

## 7.0 RECOMMENDATIONS

- a. To elaborate the region of the plasma and the plasma itself, it will be necessary to incorporate a grid with variable  $\Delta Z$  [small  $\Delta Z$  (grid size) at plasma increasing slowly with axial distance from the plasma]. A lot of work has already been done in this regard, but full implementation has not been completed at this stage;
- b. To verify if an optimum nozzle diameter exists from the point of view of the kinetic energy of the “bullet” to try to explain some of the experimental results reported by Vijay, et.al (Ref. 2);
- c. Further work is required to find a method of visualization of the steady flow with electrical discharges as density variations in this configuration are small;
- d. More work has to be done with plasma located away from the back wall to explain some of the current experimental results (Ref. 2);
- e. More work is necessary to stabilize the issuing jet;
- f. A suitable  $p/\rho$  equation for atmospheric and sub-atmospheric pressures should be added to reduce numerical difficulties.

## 8.0 ACKNOWLEDGMENTS

The author are thankful to Messrs. E. Debs [previously of the Centre for Fluid Power Technology, National Research Council of Canada (NRC) and A. Magyari (visiting student from the University of Petrosani, Romania at NRC)] for their assistance during the course of this work. The investigation was partially funded by NRC.

## 9.0 REFERENCES

1. Vijay, M.M., N. Paquette and J. Remisz 1996. Electro-discharge technique for producing powerful pulsed water jets: potential & problems. *Proc. 13th International Conference on Jet Cutting Technology*. pp.195-210. BHR Group Conference Series, Publication No. 21,

- Cranfield, Bedford, England.
2. Vijay, M.M., M. Bielawski and N. Paquette 1997. Generation of powerful pulsed waterjets with electric discharges: fundamental study. *Proc. 9th American Water Jet Conference*. pp.415-430. WJTA (Water Jet Technology Association), St. Louis, USA.
  3. Hawrylewicz, B.M., Puchala, R.J. & M.M. Vijay 1986. Generation of pulsed or cavitating jets by electric discharges in high speed continuous water jets. Chapter 36, *Proc. 8th International Symposium on Jet Cutting Technology*. pp.345-352. BHRA, Cranfield, Bedford, England.
  4. Vijay, M.M. 1998. Pulsed jets: Fundamentals and applications. *Proc. 5th Pacific Rim International Conference on Water Jet Technology*. pp. 9-23. WJTSJ, Tokyo, Japan & ISWJT, Ottawa, Canada.
  5. G. Holmqvist & K.M.C. Öjmertz 1997. Process developments and apparatus for discretized abrasive waterjet milling. *Proc.9th American. Water Jet Conference*. pp.77-91. WJTA (Water Jet Technology Association), St. Louis, USA.
  6. Atanov, G.A., V. Kolomenskaya & A. Semko 1995. The electrical impulsive waterjet device. *Proc. 4th Pacific Rim International Conference on Water Jet Technology*. pp. 187-196. WJTSJ, Tokyo, Japan.
  7. Atanov, G.A., V.V. Kolomenskaja & E.S. Geskin 1998. Interrupting a steady jet by the electric discharge to get pulsed jets. Chapter 54. *Proc. 5th Pacific Rim International Conference on Water Jet Technology*. pp. 642-649. WJTSJ, Tokyo, Japan & ISWJT, Ottawa, Canada.
  8. Hamelin, F. Kitzinger, S. Pronko & G. Schofield 1993. Hard rock fragmentation with pulsed power. *Digest of Technical Chapters, 9th IEEE International Pulsed Power Conference*, IEEE, USA.
  9. Hamelin, M., L. Asikainen & F. Kitzinger 1993. Blasting with Electricity: paving the way into 21st century mining. pp. 805-812. *Innovative Mine Design for the 21st Century*, Bawden & Archibald (eds), Balkema, Rotterdam.
  10. Reś, J. & K. Kotwica 1998. The process of rock splitting by the high-pressure waterjet assisted with electrohydrodynamic method. Chapter 53. *Proc. 5th Pacific Rim International Conference on Water Jet Technology*. pp. 633-641. WJTSJ, Tokyo, Japan & ISWJT, Ottawa, Canada.
  11. Huff, C.F. and A.L. McFall 1977. Investigations into the Effects of an Arc Discharge on a High Velocity Liquid Jet. *Sandia Laboratory Report No. SAND-77-1135C*.
  12. Schulz, W.D. 1964. *Methods in Computational Physics*. Vol. 3, pp. 1. Academic Press, New York, USA.
  13. Rochester, M.C. and J.H. Brunton 1972. High speed impact of liquid jets on solids. Chapter A1, *Proc. 1st International Symposium on Jet Cutting Technology*. pp.1-24. BHRA, Cranfield, Bedford, England.
  14. Glass, I.I. 1974. *Shock Waves & Man*. The University of Toronto Press, Toronto, Canada.

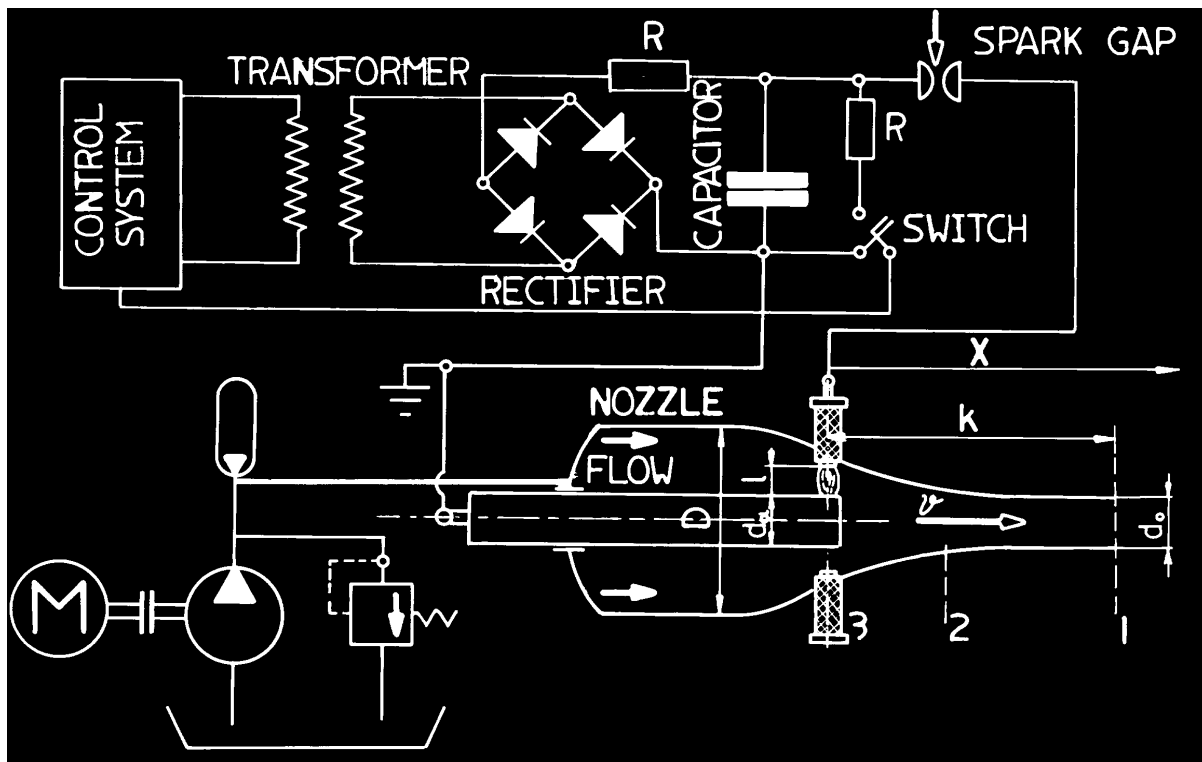


Fig. 1. A schematic diagram of the electro-discharge system for modulating a continuous stream of water for producing powerful pulsed water jets, showing electrical pulsed power system (Max: 40 kV, 20 kJ), pump (< 34.5 MPa) and a typical nozzle configuration with electrodes (Ref. 1).

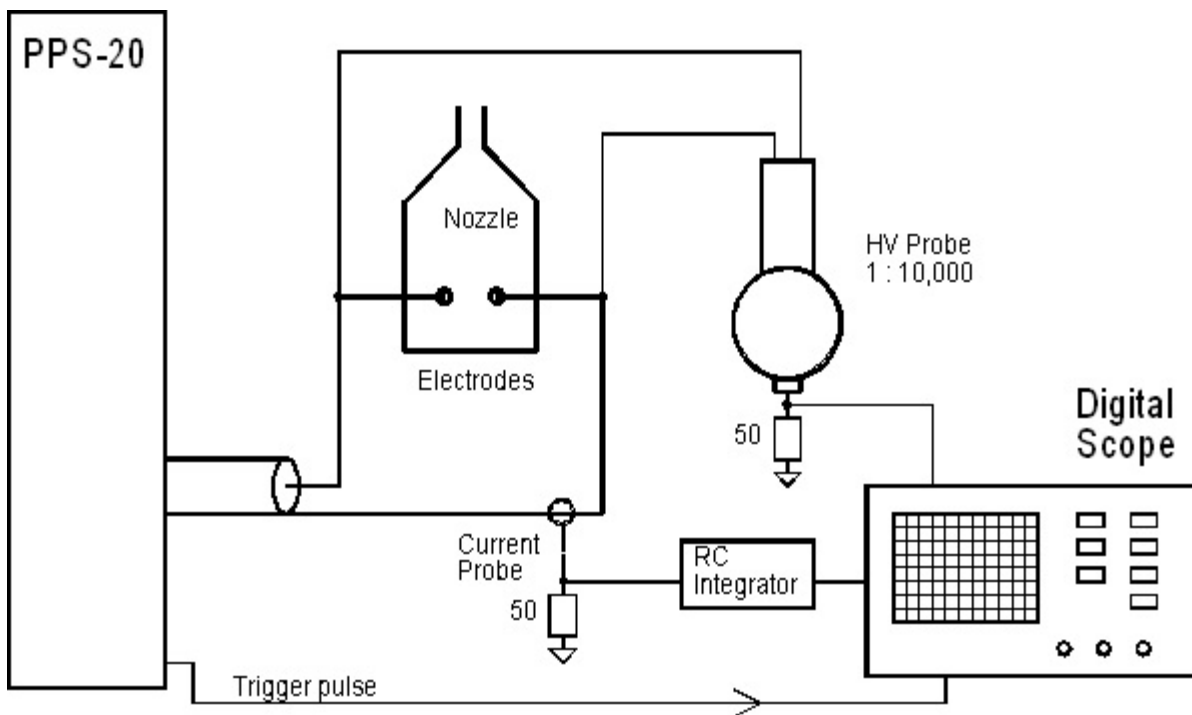


Fig. 2. A schematic diagram of the electro-discharge system for modulating a pool of quiescent water to produce a powerful pulsed jet. PPS-20: Electrical pulsed power system (Set-up for measuring the electrical parameters such as current, etc., Ref. 2).

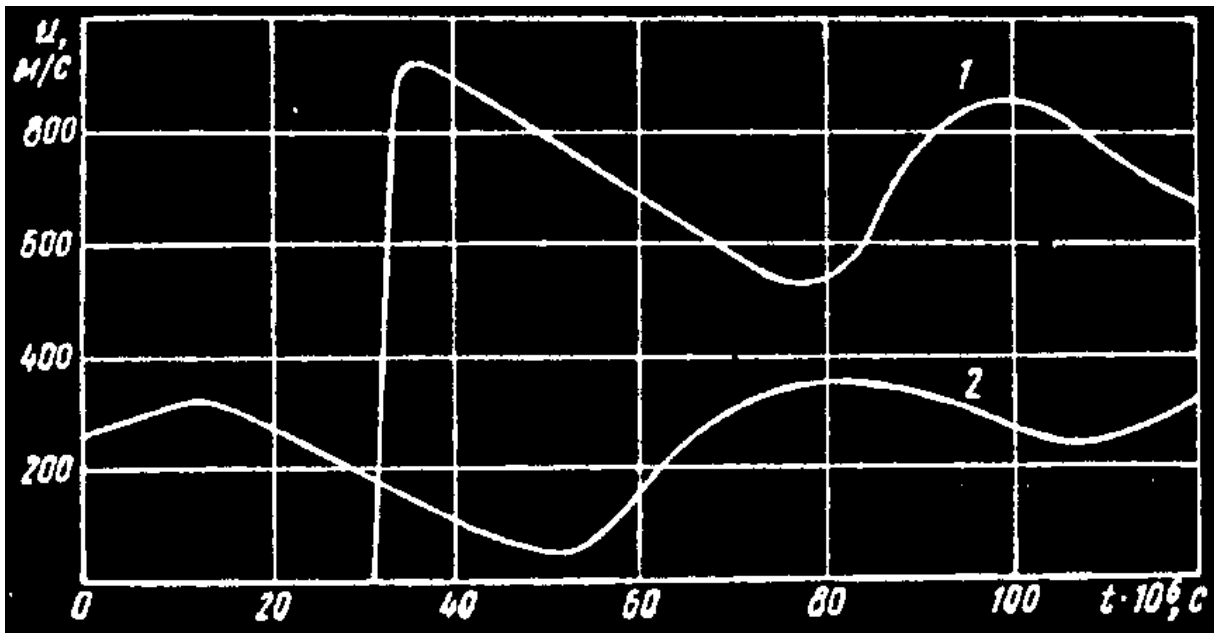


Fig. 3. Distribution of water jet velocity at the nozzle exit (curve 1) and the contact surface (bubble - water interface; curve 2) as obtained by Atanov, et. al (Ref. 6) for  $V_0 = 25$  kV,  $C = 48$   $\mu$ F,  $L = 1$   $\mu$ H,  $E_0 = 15$  kJ. Nozzle geometry consisted of  $12^\circ$  conical section with an exit diameter of 16.9 mm (no parallel section at the exit).

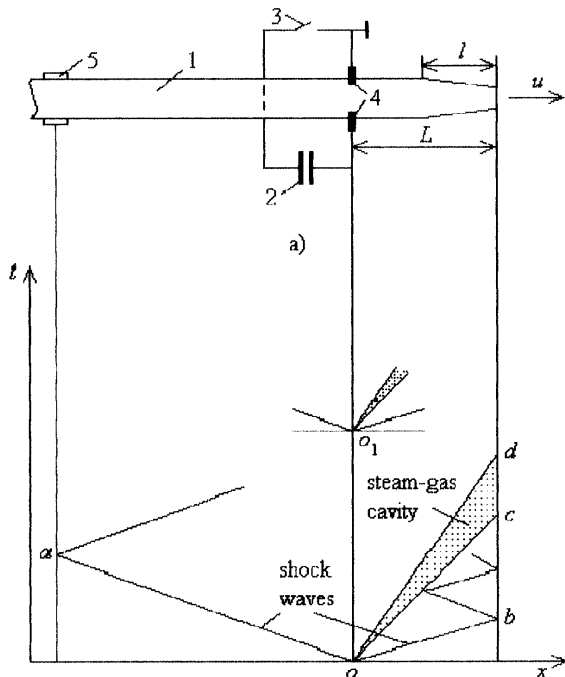


Fig. 4a. A schematic diagram of the electro-discharge technique. (a) Nozzle configuration and (b)  $x, t$  diagram of the processes accompanying the high-voltage discharge (Ref. 7).

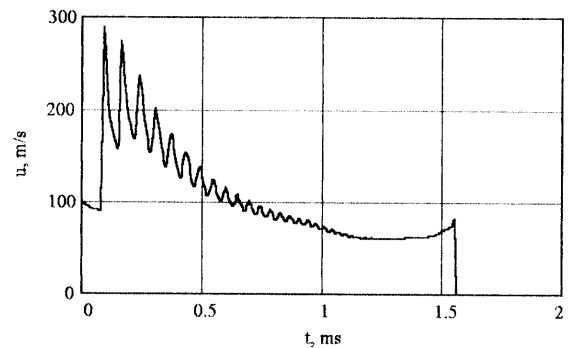


Fig. 4b. Plot of outlet speed of the jet as a function of time.  $L = 60$  mm (see Fig. 7), Initial speed of the stream = 100 m/s &  $E =$  Discharge energy = 1.15 kJ (Ref. 7).

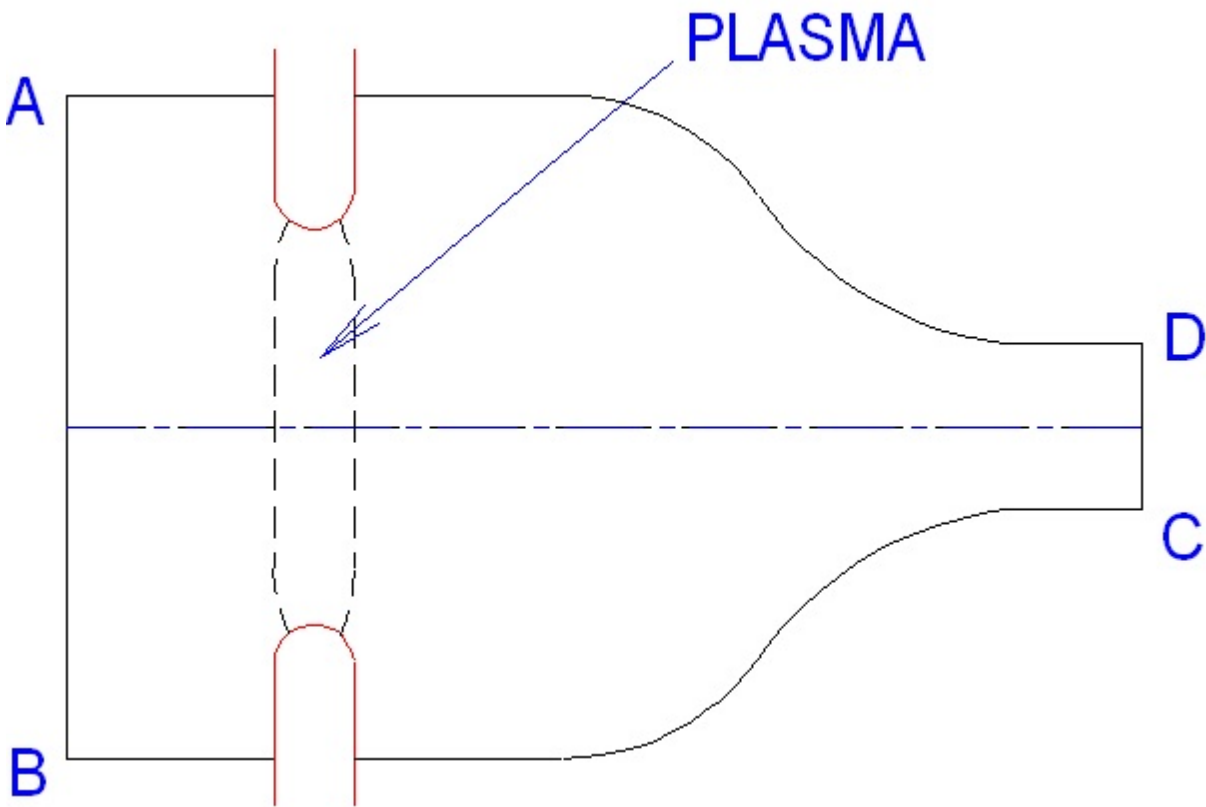


Fig. 5. A schematic sketch of the nozzle configuration used for numerical analysis showing the plasma bubble formed in the electrode gap after the electric discharge.

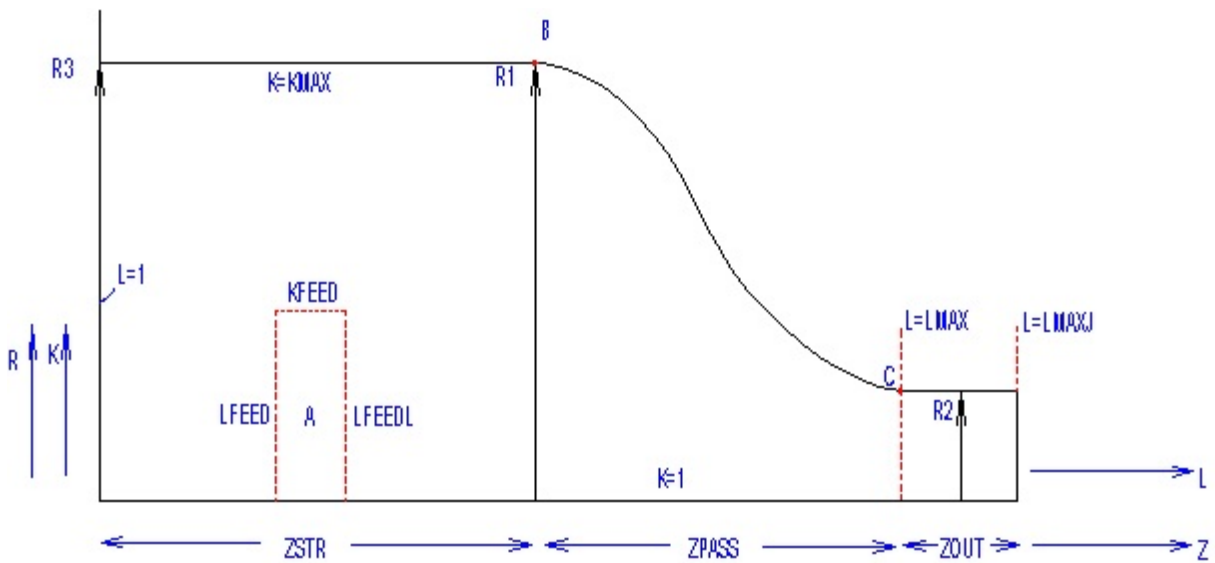


Fig. 6. Schematics of the numerical grid set up in the Lagrangian coordinates  $K$  and  $L$  running respectively in the radial and axial directions.

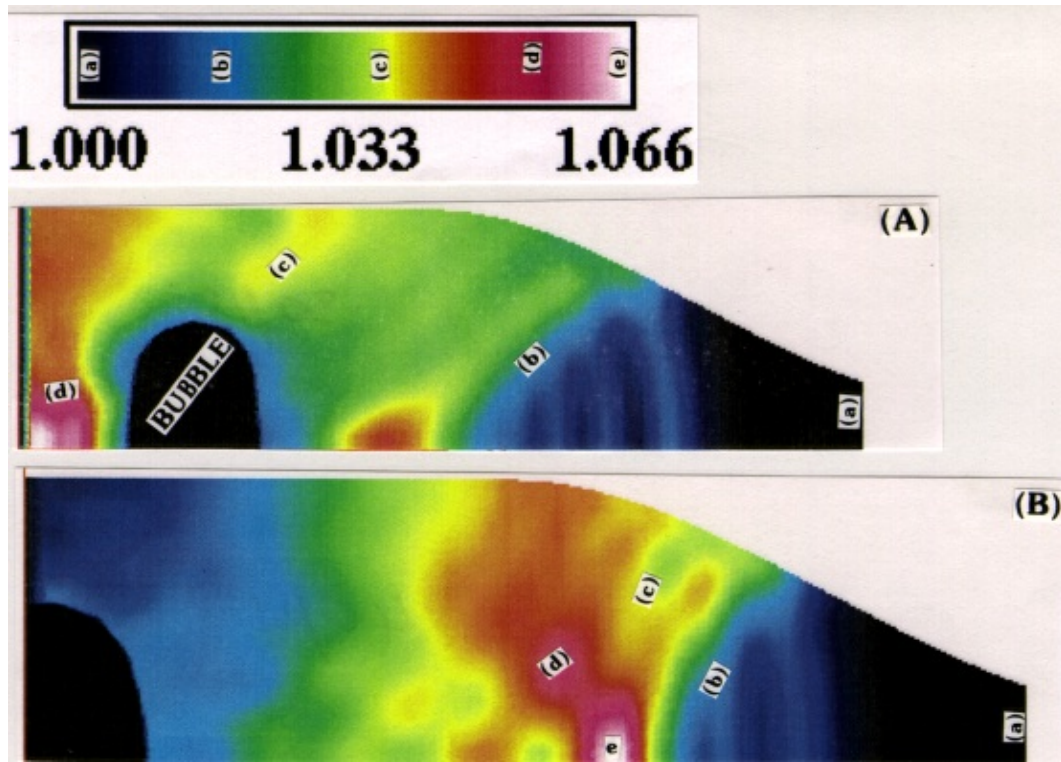


Fig. 7. Density distribution in the nozzle [indicated by “(a)”, “(b)”, etc] showing the effect of the location of the electrodes (plasma bubble). (A) 30  $\mu$ s and (B) 40  $\mu$ s after the discharge.

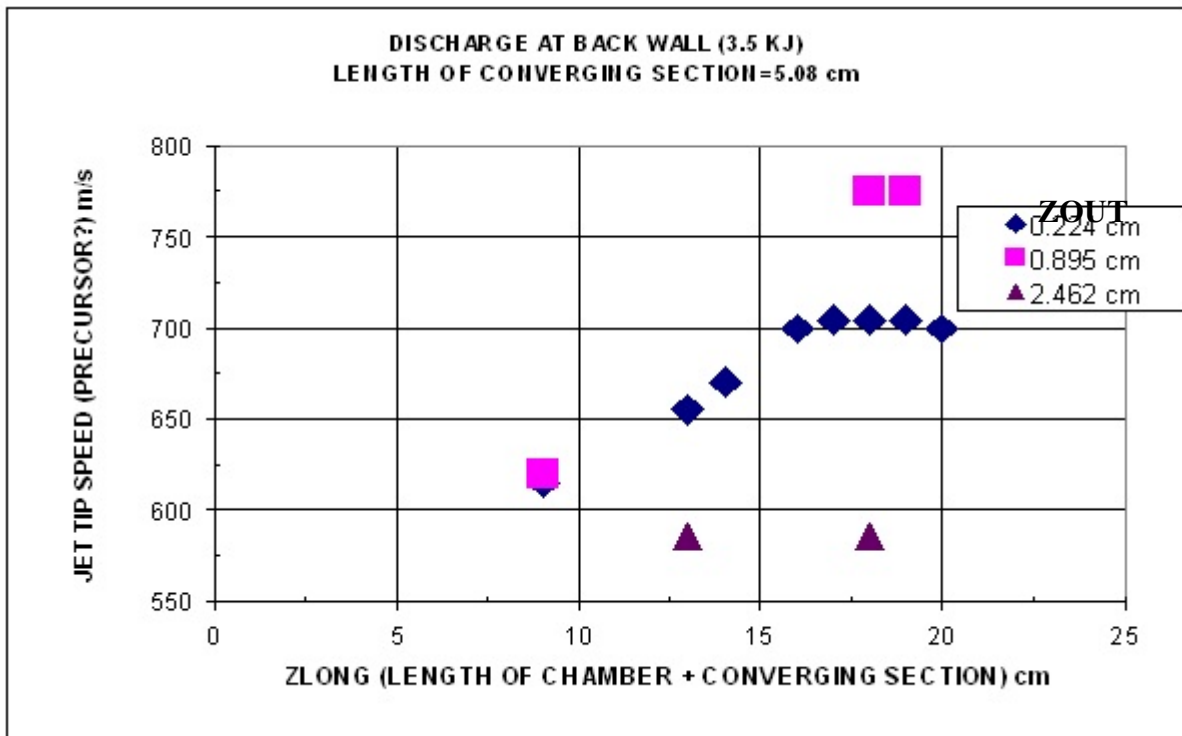


Fig. 8. Plot of local velocities which exist at the tips of the jets (presumed to be precursors). ZOUT = Length of the cylindrical part (exit) of the nozzle.

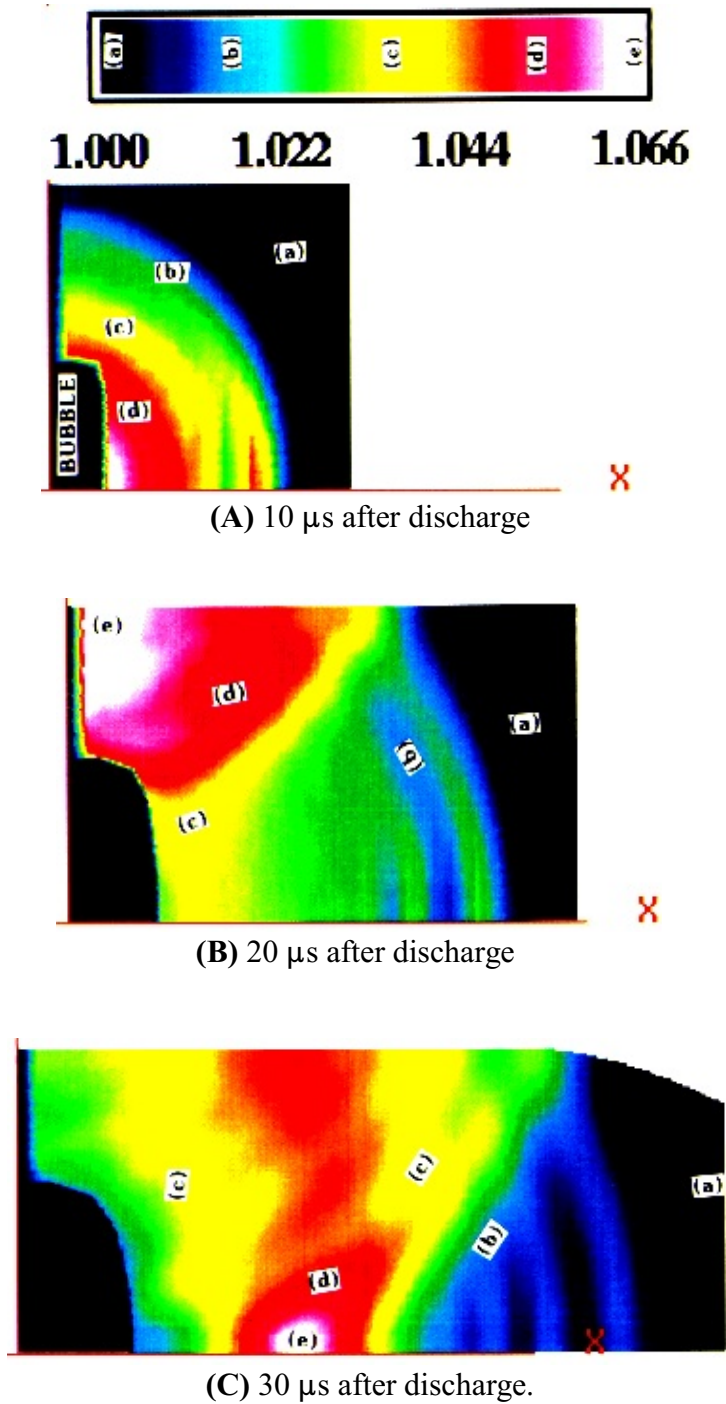
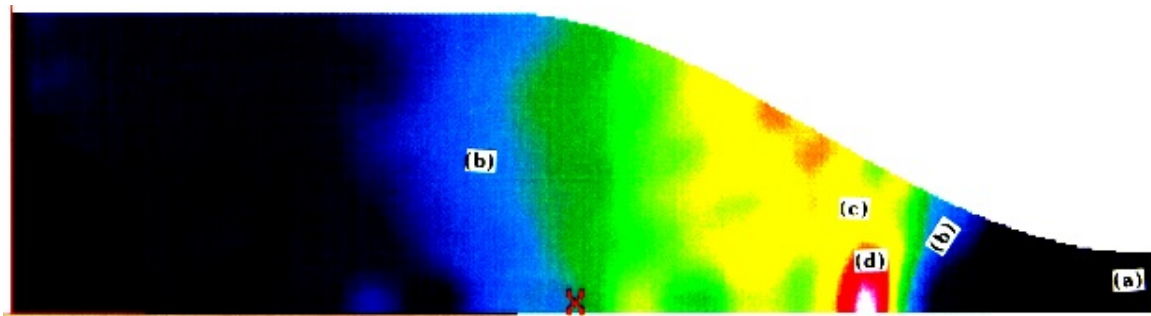
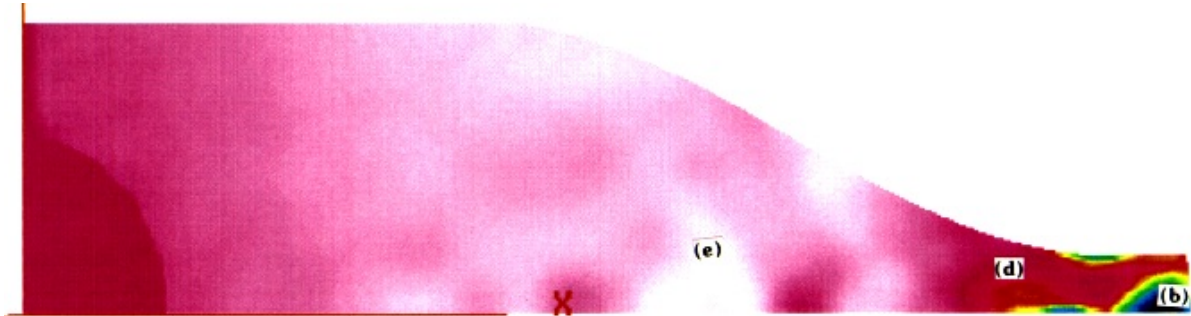


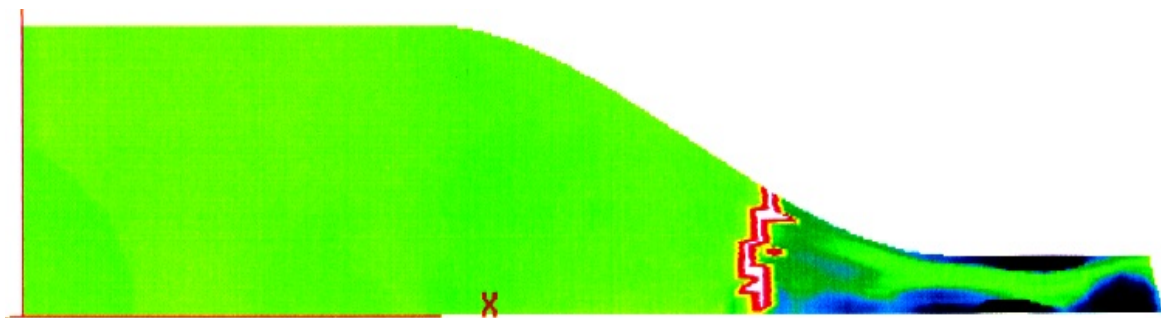
Fig. 9. Sequence of events at various times after the electrical discharge. Single-pulse jet configuration (Fig. 2). Density distribution indicated by “(a)”, “(b)”, etc.



(D) 50  $\mu\text{s}$  after discharge



(E) 70  $\mu\text{s}$  after discharge



(F) 90  $\mu\text{s}$  after discharge

Fig. 9. Continued.

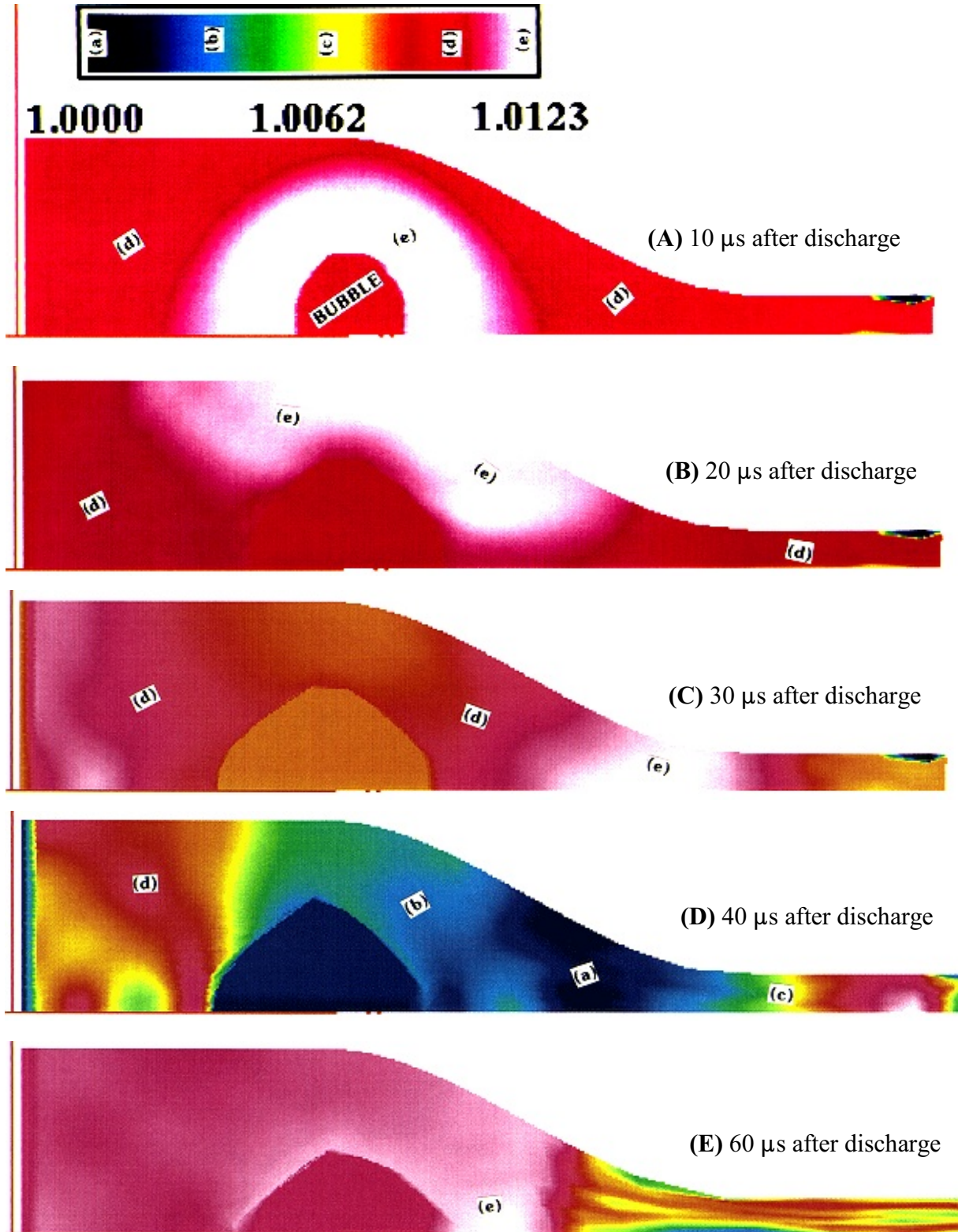


Fig. 10. Sequence of events at various times after the electrical discharge in the nozzle with steady flow (see Fig. 1). Density distribution indicated by “(a)”, “(b)”, etc.